

Nanometer-scale strain measurements in semiconductors: An innovative approach using the plasmon peak in electron energy loss spectra

A. M. Sanchez^{a)}

Departamento de Ciencia de los Materiales e IM y QI, Universidad de Cádiz, Apdo 40 E-11510 Puerto Real (Cadiz), Spain

R. Beanland

Bookham Technology, Caswell, Towcester, Northants NN12 8EQ, United Kingdom

A. J. Papworth and P. J. Goodhew

Department of Engineering, University of Liverpool, Liverpool L69 3GH, United Kingdom

M. H. Gass

Department of Materials Science and Metallurgy, Pembroke Street, University of Cambridge CB2 3QZ, United Kingdom

(Received 27 October 2005; accepted 15 December 2005; published online 2 February 2006)

We present an innovative technique for quantitative measurement of strain in semiconductor materials with high spatial resolution. The plasmon loss peak, seen in electron energy-loss spectra, has been considered following the Drude-Lorentz model, and we find that plasmon energy is extremely sensitive to lattice parameter. We have tested this model using a heterostructure of $\text{In}_{0.2}\text{Ga}_{0.8}\text{As}$ and AlAs layers in GaAs. The experimental data are in excellent agreement with the model. We estimate that strains smaller than 0.036% can be detected, corresponding to a change of $x=0.005$ in $\text{In}_x\text{Ga}_{1-x}\text{As}$, at a spatial resolution better than 2.8 nm. © 2006 American Institute of Physics. [DOI: 10.1063/1.2169904]

The properties of devices with optoelectronic and micro-electronic applications are determined to a great extent by the strain and composition of the material making up the active region of the device. There is an increasing need for analysis of strain and composition at the nanometer (nm) level as structures become smaller and more complex, often utilizing strain and/or self-assembly with layers only a few atoms thick. Transmission electron microscopy (TEM) is one of the few techniques with the spatial resolution needed for this challenge.

Here, we describe a new technique to measure strain and composition at the nm level using electron energy-loss spectroscopy (EELS) in the TEM. The technology and capabilities of EELS systems have advanced considerably in recent years,^{1–4} and it is now a routine matter to map peak positions and intensities with nm scale resolution. The most effort has been applied to analysis of core-loss edges, since these can give quantitative measurements of relative atomic concentration, although significant postprocessing is often required to extract edge intensities from a much larger background signal and signal-to-noise ratios are not ideal. However, the most significant feature in the low-loss spectrum (<50 eV) is the bulk plasmon peak, which has an intensity several orders of magnitude higher than the core-loss edges and an excellent signal-to-noise ratio. It is straightforward to measure the energy of the plasmon peak with very good accuracy; the full range of the spectrometer can be applied to only the low-loss region, giving a channel width of approximately 5 meV, and fitting a curve to the experimental data gives a robust measure of peak position and width.

The bulk plasmon is a collective oscillation of the loosely bound electrons, which runs as a longitudinal wave through the volume of the crystal with a characteristic frequency. The simplest description of the bulk plasmon is the Drude model,⁵ which gives a free-electron plasma energy E_p :

$$E_p = \hbar \omega_p = \hbar \left(\frac{ne^2}{\epsilon_0 m_0} \right)^{0.5}, \quad (1)$$

where n is the density of valence electrons, e is the electron charge, ϵ_0 is the permittivity of free space, and m_0 is the electron rest mass. The only parameter that depends upon material properties is the electron density n , given by the mean valence of the atoms and the lattice parameter. In a single crystal semiconductor heterostructure, the mean valence of the atoms is constant, and in this simple model changes in plasmon energy are only due to variations in lattice parameter.

In practice a more sophisticated approach is needed, even though damping of the oscillation can be taken into account to produce the Lorentzian shape of the plasmon energy loss peak. This is because other charges, mobile and immobile, have a significant effect on the plasmon energy. Furthermore, in any real experiment momentum transfer between the incident electron and plasmon (i.e., dispersion) will have an effect.⁶ This is responsible for the differences in plasmon energy seen with different collection aperture sizes and when the aperture is moved off the optical axis.^{7,8}

The band structure and immobile charges can be taken into account by using a Drude-Lorentz model, which includes the effect of free carriers as a single damped harmonic oscillator with energy⁹ \bar{E}_g , and the core electrons and nuclei as an additional component in the dielectric constant¹⁰ ϵ_c . This model is applicable when the plasmon peak is well-separated from \bar{E}_g . In materials such as graphite, the electron

^{a)} Author to whom correspondence should be addressed; electronic mail: ana.fuentes@uca.es

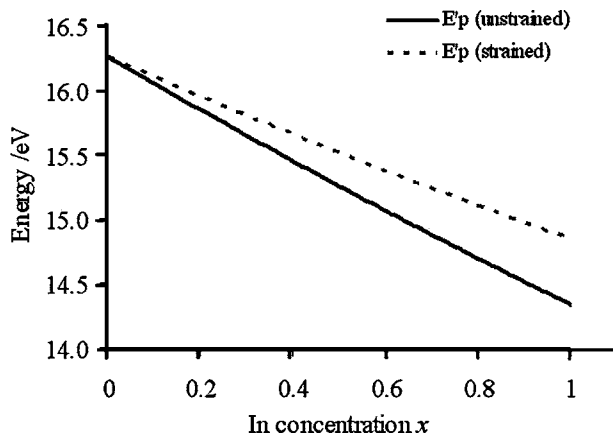


FIG. 1. The change in energy E'_p as a function of In content calculated from Eq. (3).

density has a more complex definition which must also be taken into consideration. The Drude-Lorentz model gives the maximum intensity of the plasmon energy loss peak to be¹¹

$$E_{\max} = \left[\frac{2E_p'^2 - \Gamma^2 + \sqrt{(2E_p'^2 - \Gamma^2)^2 + 12E_p'^4}}{6} \right]^{1/2}, \quad (2)$$

where Γ is a constant describing the damping of the oscillation and

$$(E_p')^2 = \bar{E}_g^2 + (E_p)^2/\epsilon_c. \quad (3)$$

The effect of damping can be removed by noting that the full width at half maximum (FWHM) of the plasmon energy loss peak is equal to Γ . Rearranging Eq. (2) to solve for $E_p'^2$, we obtain

$$E_p'^2 = E_{\max} \sqrt{4E_{\max}^2 + \Gamma^2} - E_{\max}^2. \quad (4)$$

And so by measuring the FWHM Γ and the energy of the peak E_{\max} , the parameter E_p' can be obtained from the experimental data. These equations may be used as a framework which allows experimental plasmon loss measurements to be interpreted in a quantitative manner. However, to do this some assumptions must be employed. First, we take \bar{E}_g to be the energy of the maximum absorption of an electromagnetic wave, i.e., 5.0 eV for GaAs and 3.3 eV for InAs,¹² with a linear variation between the two for $\text{In}_x\text{Ga}_{1-x}\text{As}$. For AlAs we have also taken $\bar{E}_g = 5.0$ eV. Second, we take account of peak shift due to dispersion and the immobile charges by applying Eq. (3) to data from GaAs to obtain an “effective” value of ϵ_c . This is somewhat unsatisfactory in that dispersion effects should be extracted from the data in a more rigorous fashion and are unrelated to the core dielectric constant. However, this is justified since neither dispersion nor core dielectric constant are expected to vary significantly, and we are interested in the change in plasmon energy relative to GaAs rather than an absolute value. Figure 1 shows how E_p' is expected to vary as a function of composition for $\text{In}_x\text{Ga}_{1-x}\text{As}/\text{GaAs}$. It is simplest to consider the two extremes which may occur: a pseudomorphically strained layer, in which the in-plane lattice parameters are constrained to be equal to that of GaAs and that perpendicular to the interface is enlarged due to the Poisson effect; or a completely relaxed layer which has the natural lattice parameter of $\text{In}_x\text{Ga}_{1-x}\text{As}$. The actual lattice parameter in a thin cross-section TEM specimen may be expected to lie somewhere between these

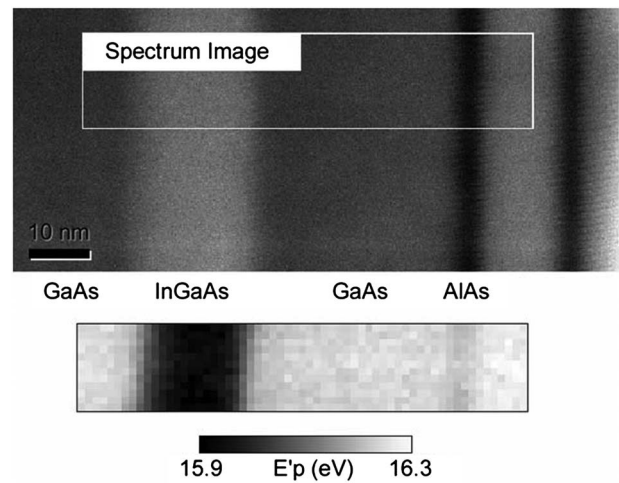


FIG. 2. Dark-field STEM image of the heterostructure indicating the area corresponding to the spectrum image. The map of E'_p is shown below.

two extremes, depending upon the $\text{In}_x\text{Ga}_{1-x}\text{As}$ layer thickness and specimen thickness. If the $\text{In}_x\text{Ga}_{1-x}\text{As}$ layer thickness is much greater than that of the specimen, the large area of free surfaces will allow almost complete relaxation and the solid curve should apply, with a shift of -19 meV for a 1% increase in the In content. On the other hand, a thin layer in a thick specimen is much closer to the situation in bulk material and the dotted curve is more relevant, with a shift of -14 meV for a 1% increase in In content. These calculations show that the plasmon peak position should be very sensitive to changes in lattice parameter; a 1% change in indium content corresponds to a change in bulk lattice parameter of 0.4 pm.

To check the validity of this technique we analysed a GaAs-based heterostructure containing an $\text{In}_{0.2}\text{Ga}_{0.8}\text{As}$ layer and two AlAs layers. The study was performed using a VG HB601 UX FEG-STEM operating at 100 kV, equipped with the Gatan ENFINA™ parallel EELS system. Energy resolution was determined to be 0.35 eV as measured from the FWHM of the zero electron energy loss peak. A collection aperture semiangle of 1.34 mrad was used, since it gives significantly increased energy resolution.¹³ Typical dwell times were 300 ms, giving a plasmon peak intensity from GaAs of ~ 2000 counts, depending on specimen thickness. The electron probe size was 0.8 nm FWHM, with ~ 1 nm spacing between data points. Single scattering distributions were derived from the raw spectra using a Fourier-log deconvolution method.

Experimental variations in plasmon energy was estimated using many large area maps of GaAs, containing ~ 800 spectra. In this data set the standard deviation of the fitted plasmon energy was 7 meV. Since a 1% change in indium content gives a shift of 14–19 meV, very small changes in composition should be distinguishable. Plasmon energy is relatively insensitive to specimen thickness,¹⁴ although significant changes are present in very thin specimens (< 25 nm).¹⁰

The upper part of Fig. 2 shows a dark-field Scanning transmission electron microscopy (STEM) image of the heterostructure. The specimen thickness was determined to be ~ 40 nm based on a Kramers-Kronig analysis. A spectrum image of the low-loss region was recorded in the marked area, and the resulting map of E'_p is shown below.

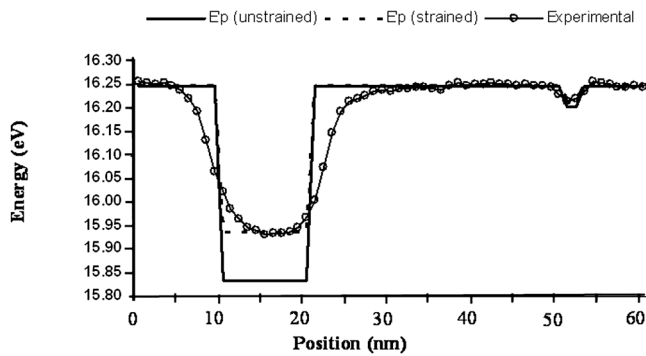


FIG. 3. Comparison between theoretical and experimental energies E'_p .

Using Eq. (3), we may compare the theoretical and observed plasmon peak energies. Figure 3 shows an averaged line plot of the experimental data (open circles) and predicted peak energies for a perfectly abrupt structure which is pseudomorphically strained (dashed line) and relaxed (solid line). Thus there is excellent agreement with the values expected for the strained layer. In the centre of the $\text{In}_{0.2}\text{Ga}_{0.8}\text{As}$ layer, the experimental peak shift of 328 meV lies close to the strained value (309 meV), as would be expected for a 15-nm-thick layer in a 40-nm-thick specimen. A similar effect can be observed in the 3 nm AlAs layer.

These data show that the technique clearly has the sensitivity to changes in lattice parameter to be a useful technique. It is also apparent that the spatial resolution of the technique is very high. We have estimated spatial resolution by assuming a perfectly abrupt structure and approximating the interaction of the beam and sample as having as a Gaussian profile. Varying the radius of this Gaussian until a good fit is obtained with the shape of the $\text{In}_{0.2}\text{Ga}_{0.8}\text{As}/\text{GaAs}$ interface in Fig. 3 gives a best fit at a radius of 2.8 nm. The observed resolution is almost exactly as expected by the formula for spatial resolution (τ (nm)) = $40/E$ (eV).¹⁵ We believe the actual resolution to be even higher, since the structure is not truly abrupt and some degradation of the image is visible in Fig. 1 due to external electromagnetic fields. This is better than expected from some calculations, which show that delocalisation should significantly reduce spatial resolution of low-loss images¹⁶—a finding we have in common with other low-loss studies.^{17,18}

In summary, we have demonstrated that plasmon peak shifts can be used to determine local strains at a nm scale. We expect that this approach should be viable for a wide range of materials including $\text{Si}_x\text{Ge}_{1-x}$, and III-nitrides, as one of the characteristic properties of a semiconductor energy loss spectrum is a single, well-defined and intense plasmon peak.

A.M.S. would like to acknowledge financial support from EPSRC and SANDIE European Network of Excellence (NNPA-CT-2004-500101, Sixth Framework Program) for many aspects of this work and M. Kundmann for providing his Ph.D. thesis.

- ¹R. Brydson, A. V. K. Westwood, X. Jiang, S. J. Rowen, S. Collins, A. Lu, B. Rand, K. Wade, and R. Coult, *Carbon* **36**, 1139 (1998).
- ²V. J. Keast, *J. Electron Spectrosc. Relat. Phenom.* **143**, 97 (2005).
- ³Y. Y. Lei, Y. Ito, N. D. Browning, and T. J. Mazanec, *J. Am. Ceram. Soc.* **85**, 2359 (2002).
- ⁴M. H. Gass, A. J. Papworth, T. J. Bullough, and P. R. Chalker, *Ultramicroscopy* **101**, 257 (2004).
- ⁵P. Drude, *Phys. Z.* **14**, 161 (1900).
- ⁶H. Raether, *Excitation of Plasmons and Interband Transitions by Electrons* (Springer, Berlin, 1980).
- ⁷O. L. Krivanek, M. K. Kundmann, and K. Kimoto, *J. Microsc.* **180**, 277 (1991).
- ⁸R. F. Egerton, *Electron Energy Loss Spectroscopy in the Electron Microscope* (Plenum, New York, 1986).
- ⁹P. Schattschneider and B. Jouffrey, in *Energy-Filtering Transmission Electron Microscopy*, edited by L. Reimer (Springer, Berlin, 1995).
- ¹⁰M. K. Kundmann, Ph.D. thesis, University of California, Berkeley, California (1988).
- ¹¹A. M. Sánchez, R. Beanland, M. H. Gass, A. J. Papworth, P. J. Goodhew, and M. Hopkinson, *Phys. Rev. B* **72**, 075339 (2005).
- ¹²*Properties of Gallium Arsenide*, 2nd ed. (Inspec, London, 1990).
- ¹³A. C. Ferrari, A. Libassi, B. K. Tanner, V. Stolojan, J. Yuan, L. M. Brown, S. E. Rodil, B. Kleinsorge, and J. Roberson, *Phys. Rev. B* **62**, 11089 (2000).
- ¹⁴R. Beanland, A. M. Sanchez, A. J. Papworth, M. H. Gass, and P. J. Goodhew, in *Microscopy of Semiconducting Materials 2005*, Institute of Physics Conference Series (in press).
- ¹⁵L. M. Brown, in *Impact of Electron and Scanning Probe Microscopy on Materials Research*, NATO Science Series Vol. 364, edited by D. Rickertby, G. Valdre, and U. Valdre (Kluwer, Dordrecht, 1999).
- ¹⁶O. L. Krivanek, M. K. Kundmann, and K. Kimoto, *J. Microsc.* **180**, 277 (1991).
- ¹⁷H. R. Daniels, R. Brydson, A. Brown, and B. Rand, *Ultramicroscopy* **96**, 547 (2003).
- ¹⁸A. R. Lupini and S. J. Pennycook, *Ultramicroscopy* **96**, 313 (2003).